The nature and kinetics of 2,4-dimethylphenol adsorption in aqueous solution on biochar derived from *Sargassum boveanum* macroalgae

Mazen K. Nazal, Durga Rao and Nabeel Abuzaid

ABSTRACT

Many industries produce 2,4-dimethylphenol (DMP) compound in the wastewater which is persistent, toxic, and carcinogenic. Therefore, an adsorbent was prepared by carbonizing a dried *Sargassum boveanum* macroalgae. The prepared biosorbent was investigated for adsorptive removal of DMP from aqueous solution. After carbonization, the biochar derived from *S. boveanum* macroalgae (BCM) removed almost 100% of DMP adsorbate. Effects of contact time, solution pH, adsorbate concentration, adsorbent mass, and temperature have been studied. It has been found that, within the experimental conditions, the maximum adsorption capacity is 17 mg/g, rate of adsorption follows pseudo-second order kinetics and the adsorption isotherm experimental data fit the Freundlich model. The thermodynamic parameters were calculated and it has been found that the adsorption of DMP on BCM is endothermic and thermodynamically favorable, and in addition the surface of BCM adsorbent shows affinity to the DMP molecules. The BCM adsorbent has the capability to remove around 65% of DMP from high saline seawater contaminated with DMP. Moreover, the prepared BCM adsorbent was reusable for at least four times in seawater for removal of DMP contaminant.

Key words | adsorption isotherms, environment, phenolic compounds, removal efficiency, thermodynamics of adsorption, wastewater treatment

Mazen K. Nazal (corresponding author)
Durga Rao
Nabeel Abuzaid
Center for Environment and Water,
Research Institute, King Fahd University of Petroleum and Minerals,
Dhahran 31261,
Saudi Arabia
E-mail: *mazennazal@kfupm.edu.sa*

HIGHLIGHTS

- Improved the removal efficiency of macroalgae after the carbonization.
- High removal efficiency of DMP from aqueous solution of 100% was obtained.
- Investigated the isotherm, kinetics and thermodynamics of DMP adsorption.
- The adsorption process of DMP molecules is spontaneous and thermodynamically favorable.
- The adsorption process of DMP molecules is endothermic with a negative $\Delta H = 108.1$ kJ mol^{-1}.
- The prepared BCM adsorbent is reusable for at least four times for DMP removal from seawater.

INTRODUCTION

The effluents of different industries such as petrochemical, oil refining, plastics, pharmaceuticals, insecticides, fungicides, dyes, and rubber chemicals are the major source of phenol pollutants (Mohammadi *et al.* 2015; Sun *et al.* 2015). Owing to their high toxicity, persistence, and possible bioaccumulation in the environment, they have been listed as pollutants of priority concern by the US Environmental Protection Agency (USEPA) and they have received special attention from scientists and researchers. Discharging these compounds without treatment not only contaminates

doi: 10.2166/aqua.2020.142

drinking water and groundwater but also seawater and different aquatic environments which lead to serious health risks to animals, aquatic systems, as well as humans (Snoeyink *et al.* 1997; Sun *et al.* 2015). Therefore, there are many proposed methods for treatment of contaminated water which contains phenol compounds. These methods are (i) chemical oxidation, (ii) biodegradation, (iii) adsorption, (iv) membrane separation, (v) ion exchange, (vi) solvent extraction, (vii) ozonation, (viii) electrochemical oxidation, etc. (Ahmaruzzaman 2008; Laura *et al.* 2016). Among these methods, the adsorption process is one of the most efficient and promising methods applied widely for removal of contaminants from water bodies, and is simple, low cost, and capable of removing most forms of organic substituted phenol compounds (Li *et al.* 2015). This has led to researchers having more interest to develop adsorbent from different sources which are more efficient, cheaper, renewable, and more abundantly available than the commercially available materials such as activated carbon. Adsorption using naturally available macroalgae has shown promising results in removing many pollutants such as heavy metals (Nazal 2019) and phenolic compounds (Eugenia *et al.* 2006) from different aqueous media. These bioadsorbents are eco-friendly, inexpressive, and freely available. The brown seaweed macroalgae (*Phaeophyta*) are a potential source of bioadsorbent. One of these brown seaweeds are the *Sargassum boveanum* macroalgae which are abundant and freely available in the Arabian Gulf coastal area. They have many advantages as a bioadsorbent due to their cell wall structure and components, which contains cellulose, alginate, and other polysaccharides. These compounds have many chemical functional groups such as carboxylic acid, hydroxyl, and amine that could be active adsorption sites with high affinity, capacity, and selectivity to phenolic compounds. In addition, bioadsorption of phenolic compounds using brown macroalgae could be achieved through hydrophobic and donor–acceptor interactions (Podgorskii *et al.* 2004). Moreover, modifying the macroalgae by deriving a biochar and activating their surface and structure is also expected to improve their adsorption capacity for removal of phenolic compounds.

To the best of our knowledge, there is no information available concerning the adsorption of 2,4-dimethylphenol (DMP) compound onto a biochar adsorbent derived from *S. boveanum* marine macroalgae. Therefore, in this study, a biochar from *S. boveanum* macroalgae was prepared, characterized, then used as a biosorbent for the removal of DMP phenolic compound from aqueous solution. The effect of adsorption conditions such as the solution pH, adsorbent mass, and adsorbate concentration were investigated. The adsorption isotherms were studied by fitting the experimental data with the common isotherm models. The adsorption kinetics for this phenolic compound were studied. In addition, the thermodynamic parameters for the DMP adsorption on the prepared adsorbent were calculated and the reusability of the adsorbent for the removal of DMP from seawater was also tested.

EXPERIMENTAL

Materials

2,4-dimethylphenol (DMP) was selected for the current study. All chemicals were analytical reagent (AR) grade and purchased from Chem Service, Inc., USA. Dichloromethane (99.9% purity, Fisher German) and a deionized water were used.

Preparation and characterization of adsorbent

The *S. boveanum* macroalgae (MA) were collected from the Arabian Gulf coastal area and washed thoroughly with tap water then by distilled water to remove the water-soluble impurities. The washed material was dried at 110 °C for 48 hours. A biochar-derived *S. boveanum* macroalgae (BCM) was prepared by carbonizing the clean MA in a tube furnace at 500 °C under argon atmosphere (inert gas) and heating rate of 10 °C/min for 2 hours then cooled down to room temperature. The prepared adsorbent was preserved in a tightly closed vial for characterization and later for use in the adsorption experiments.

The functional groups on the surface of MA and BCM adsorbents were identified using the Fourier transform infrared (FTIR) (Nicolet 6700 Thermo Electron) instrument, and the thermal stability of the material under air and nitrogen was tested using thermal gravimetric analysis (TGA Q500, TA Instruments, USA). The adsorbent's surface morphology

and its elemental composition were characterized using a scanning electron microscope coupled with energy dispersive X-ray (SEM-EDX) (Jeol 6700LV). An automated gas sorption analyzer (Autosorb iQ Quantachrome USA) was used to analyze the surface area and porosity of the adsorbent.

Preparation of adsorbate solution

A stock solution of DMP (1,000 mg/L) was prepared in deionized water. Subsequent test solutions were prepared by appropriate dilution of the stock solution with deionized water for the adsorption experiments or seawater to approach the real application. The pH of the test solutions was adjusted using nitric acid HNO_3 (2 M) and potassium hydroxide KOH (1 M), and the pH was measured using a pH meter (model PC 2700, Oakton Instruments, USA).

Analytical method

The DMP molecules were extracted from 5 mL of the filtered aqueous sample, before and after the adsorption, using 5 mL of dichloromethane solvent, then a 1 μL from the extract was analyzed using a gas chromatography coupled with flame ionization detector (GC-FID) instrument (Agilent Technology 6890N). The used column and the GC-FID parameters are summarized in Table 1.

Table 1 | The chromatographic conditions

Parameter	Description
Injection mode	Split-less mode
Temperature of injector	280 °C
Column	DB-1 (30 m × 0.32 mm × 1 μm) GC capillary column
Flow rate of helium	1.5 mL/min
Temperature program	Started from 40 °C for 1 minute then heated up to 300 °C with a heating rate of 10 °C/min with holding time of 1 minute
FID detector temperature	300 °C
Flow of air	300 mL/min^{-1}
Flow of hydrogen	30 mL/min
Flow of makeup gas (nitrogen)	15 L/min

Batch adsorption experiments

The adsorption of DMP on the adsorbent was studied at a shaking speed of 180 rpm using the batch mode experiment. The effect of solution pH on DMP adsorption was studied at 24 ± 0.1 °C. Ten mg/L of DMP was prepared in deionized water having different pH values (i.e., 1, 2, 5, 7, 8, and 10). 50 ± 0.1 mg of adsorbent was added to a 50 mL solution in a screw-capped conical flask then agitated for 16 h. The effect of the adsorbent dosage on the removal of DMP (20 mg/L) from its solution was investigated by varying the added mass of BCM adsorbent from 5 to 150 ± 0.1 mg at a constant temperature of 24 ± 0.1 °C for 16 h. The effect of DMP concentration (i.e., 1, 5, 10, 15, 20 30, and 40 mg/L) on its removal efficiency using 50 ± 0.1 mg of adsorbent was studied at 24 ± 0.1 °C. For studying the adsorption kinetics of DMP (15 mg/L), 50 ± 0.1 mg of adsorbent were used for different time intervals from 5 to 960 minutes. The adsorption thermodynamics of DMP (5 mg/L) on 50 ± 0.1 mg of adsorbent was studied at different temperatures (i.e., 24, 30, 35, 40, 50, and 60 ± 0.1 °C). For approaching the real environmental application, 200 ± 0.1 mg of BCM adsorbent was used for decontaminating seawater that had 30 mg/L of DMP pollutant. Finally, the reusability of the prepared BCM adsorbent for removing DMP from seawater was evaluated for four cycles. In all the experiments, the samples were filtered using Whatman filter papers 42 to remove the adsorbent. To estimate the loss of DMP due to the evaporation or adsorption on the wall of the conical flask, control samples were placed together with the test samples in a water bath shaker (BS-31, Lab Companion, Korea). In each experiment, these samples had the same tested concentration and pH of the DMP solution but without adsorbent. The results of the control samples showed that there was no loss of DMP due to the experimental procedure. The precision of experiments was estimated by calculating the RSD % for five replicates of the test samples and it was 10.9%.

The adsorbed amount of DMP on the adsorbent (q_e) in mg/g unit was calculated using Equation (1):

$$q_e = \frac{(C_o - C_e)}{m} \text{ x } V \quad (1)$$

where C_o is the initial concentration (mg/L) of DMP compound, V is the volume (L) of solution, and m is the mass (g) of adsorbent. The percentage of removal (%) was calculated using Equation (2):

$$Removal\ \% = \frac{C_o - C_e}{C_o} \times 100 \tag{2}$$

Adsorption isotherms

The equilibrium data of DMP adsorption on the adsorbent was tested by various frequently used adsorption isotherm models. The Freundlich isotherm (Freundlich 1906), presented in Equation (3), is an empirical model that was established by assuming the surface of the adsorbent is heterogeneous and the adsorption sites have different affinities to the adsorbate molecules. It also describes the multilayer adsorption and assumes the adsorption process is reversible.

$$q_e = K_F C_e^{1/n} \tag{3}$$

Equation (4) shows the linear form of the Freundlich isotherm model.

$$\ln(q_e) = \ln(K_F) + \frac{1}{\mathrm{n}} \ln(C_e) \tag{4}$$

where K_F and n are the Freundlich parameters, n is a measure of the heterogeneity of the surface of the adsorbent.

The Langmuir isotherm model (Langmuir 1916), presented in Equation (5), assumes a monolayer of adsorbate is formed on the surface of the adsorbent and there is no interaction or steric hindrance between the adsorbate molecules, as well as all the adsorption sites on the surface of the adsorbent being identical with the same activation energy adsorption.

$$q_e = \frac{(Q_o b\ C_e)}{(1 + b\ C_e)} \tag{5}$$

The linearized form of the Langmuir isotherm is presented in Equation (6):

$$\frac{1}{q_e} = \frac{1}{Q_o} + \frac{1}{bQ_oC_e} \tag{6}$$

where Q_o in mg/g is the monolayer maximum adsorption capacity and b is the Langmuir constant.

The dimensionless separation factor (R_L) obtained from the Langmuir equation is given in Equation (7):

$$R_L = \frac{1}{(1 + b\ C_o)} \tag{7}$$

If the value of R_L is 0 then the adsorption is reversible, $0 < R_L < 1$ favorable, $R_L = 1$ linear, and if $R_L > 1$ this indicates the adsorption is unfavorable.

Temkin is another model that contains a factor describing the interaction between the adsorbate and adsorbent (Temkin & Pyzhev 1940). Equations (8) and (9) represent the Temkin isotherm model and its linear form, respectively:

$$q_e = \frac{\mathrm{RT}}{b_T} \ln A_T \mathrm{C_e} \tag{8}$$

$$q_e = \frac{RT}{b_T} lnA_T + \frac{RT}{b_T} lnC_e \tag{9}$$

where b_T is the Temkin constant, R and T are the ideal gas constant in J K^{-1} mol^{-1} and the temperature in Kelvin (K), respectively, and A_T is the isotherm adsorption constant in L/g which gives an idea about the adsorption capacity.

In the above-mentioned isotherm models, q_e is the adsorption capacity at equilibrium in mg/g, C_e is the concentration of DMP in the solution at equilibrium in mg/L.

Two functions were used to evaluate and later to determine the best isotherm model fitting the adsorption experimental data: they are the summation of relative error (SRE) between the experimental adsorption capacity ($q_{e\,exp.}$) and the predicted adsorption capacity ($q_{e\,pred.}$) and the squared correlation coefficient (R^2) that are shown, respectively, in Equations (10) and (11):

$$SRE = \sum_{i=0}^{n} \left[\frac{(q_{e\,exp.} - q_{e\,pred})_i^2}{q_{e\,exp}} \right] \tag{10}$$

$$R^2 = \frac{\sum_{i=0}^{n} (q_{e\,exp} - \overline{q_{e\,pred}})_i^2}{\sum_{i=0}^{n} (q_{e\,exp} - q_{e\,pred})_i^2 + \sum_{i=0}^{n} (q_{e\,exp} - \overline{q_{e\,pred}})_i^2} \tag{11}$$

where $\overline{q_{e\,pred}}$ is the average predicted equilibrium adsorption capacity.

Adsorption kinetics

To study the DMP adsorption kinetics on BCM adsorbent, the adsorption results were fitted using the kinetic models represented in Equations (12)–(14) for, respectively, a pseudo-first order adsorption rate (Lagergren 1898),

$$ln(q_e - q_t) = ln(q_e) - k_1 t \tag{12}$$

a pseudo-second order adsorption rate (Ho & McKay 1998),

$$\frac{t}{q_t} = \frac{1}{q_e^2 k_2} + \frac{t}{q_e} \tag{13}$$

and Elovich kinetic model (Chien & Clayton 1980), which is considered one of the most useful models for describing chemical adsorption:

$$q_t = \left(\frac{1}{b}\right) \ln ab + \left(\frac{1}{b}\right) \ln q_t \tag{14}$$

where q_t in mg/g is the adsorption capacity at a time t (min), k_1 (min^{-1}) is the pseudo-first order rate constant, and k_2 (g mg^{-1} min^{-1}) is the pseudo-second order rate constant. In the Elovich model, a is the initial sorption rate (mg g^{-1} min^{-1}) and b is the desorption constant (g/mg) during experiment.

RESULTS AND DISCUSSION

Characterization of the adsorbents

To gain an insight into the thermal stability of MA and BCM adsorbents in a temperature range from 25 to 800 °C, the thermal analysis was performed using a titanium pan with a sample weight of 15 mg under air with a flow rate of 30 mL/min and heating rate of 10 °C/min. The same experiment was carried again out under an inert atmosphere (nitrogen gas) to show the weight loss percentage in MA during the BCM preparation. Figure 1 shows the thermal oxidation and degradation of MA and BCM adsorbents under air and nitrogen atmosphere. It was found that under air MA adsorbent has three weight loss phases that are attributed to the oxidation, degradation, and decomposition. The first main step started at 213 °C and was completed at around 368 °C, with a loss of 51.2% of its original mass. The second step was in a temperature range between 424 and 482 °C with a 73.5% loss, while the third step was between 712 and 800 °C with 88.7% loss. However, BCM adsorbent shows two main oxidation and degradation steps. The first one started at around 344 °C and was completed at around 520 °C with a weight loss of 40%. The second degradation step was in a temperature range between 721 and 800 °C with a weight loss of 57.7%. Under nitrogen, the decomposition of MA material was between 211 and 800 °C with a weight loss around 75%, while for BCM adsorbent, its decomposition was between

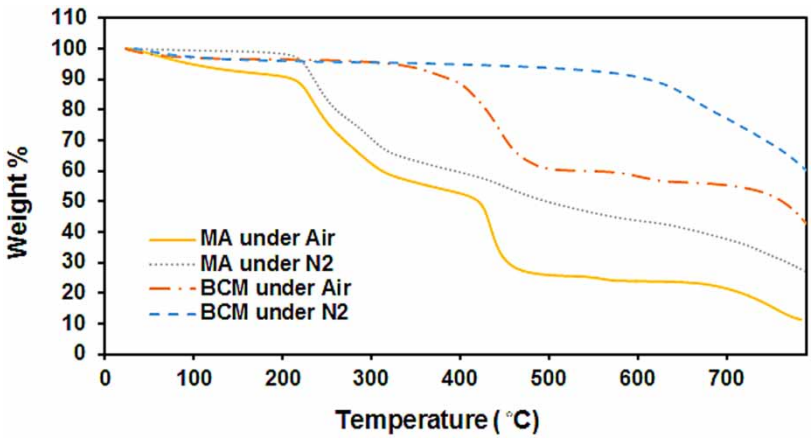

Figure 1 | Temperature versus weight % of MA and BCM adsorbents under air and nitrogen (N2) atmosphere.

600 and 800 °C with a weight loss around 41%. It may be concluded that the BCM shows more thermal stability under both atmospheres.

The functional groups on the surface of the adsorbents were identified using FTIR experiment. Figure 2 shows the IR spectra for the raw and carbonized macroalgae. The macroalgae contain cellulose, polysaccharides, fucoidans, alginates, and proteins. The absorption between 3,600 and 3,000 cm^{-1} is due to the stretching, vibration and angular vibration of hydroxyl (OH) and amine (NH_2) groups. The weak and intense absorption bands in the ranges of 1,500 to 1,300 cm^{-1} and 1,640 to 1,540 cm^{-1} are due to the presence of proteins (Sekkal *et al.* 1993). However, their precise assignment is difficult because of the complexity of protein structures. The intense band between 1,000 and 1,100 cm^{-1} is due to the presence of the polysaccharides (Ata *et al.* 2012). The intense bands at 1,100, 1,680, and 1,425 cm^{-1} are attributed to the presence of the hemiacetals and carbonyl functional groups, respectively. These functional groups confirm the presence of polyalginates, which mainly contribute to the adsorption of organic pollutants (Navarro *et al.* 2008; Cuizano *et al.* 2009). Finally, the decrease in the peak intensity at around 3,440 and 1,620 cm^{-1} and the intense absorption peak at 1,420 cm^{-1} in the BCM material are due to the carbonization.

The dried macroalgae before and after carbonization were placed on aluminum stubs and sputter-coated with gold-palladium or platinum using a DESK V HP TSC cold sputter coater. Respectively, Figures 3 and 4 show the surface morphology and the elemental composition of MA and BCM adsorbents. According to the images, the surface heterogeneity of MA adsorbent is greater than the surface heterogeneity of BCM adsorbent. The energy dispersive X-ray (EDX) results, which are presented in Table 2, show the surface of MA covered with alkali metals to be more than those on the surface of BCM. However, the carbonization of MA removed these metals and produced surface morphology with small openings and holes having a larger contact area and more active adsorption sites. Moreover, the carbon and oxygen element percentages on the surface of BCM adsorbent were found to be 61.78 and 33.85%, respectively, and they are higher than the percentages of carbon (35.56%) and oxygen (12.81%) elements on the surface of MA material before carbonization which may contribute in increasing the adsorption capacity of BCM for DMP phenolic compound (Vidic *et al.* 1993).

The surface area and pore volume of the adsorbents were obtained at relative pressures between 0.10 and 1.00. The liquid nitrogen adsorption-desorption isotherms were measured after degassing all the adsorbents at 200 °C to a pressure of 6.5×10^{-5} Torr. The Brunauer–Emmett–Teller (BET) and the density functional theory (DFT) methods were used to calculate the surface area and total pore volume, respectively. The results show the surface area of the BCM adsorbent is small (3.8 m^2/g) and the pore volume is 0.006 mL/g with an average pore size of 7.049 Å. However, that was larger than the surface area (1.34 m^2/g) and the pore volume (0.005 mL/g) of the MA material but smaller than its average pore size (13.845 Å).

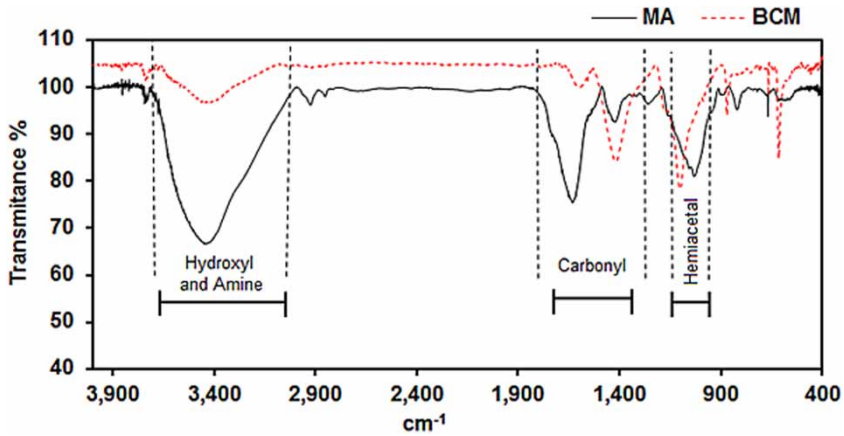

Figure 2 | FTIR spectrum of MA (solid line) and BCM (dotted line) materials. Dashed lines are to specify the main absorption bands.

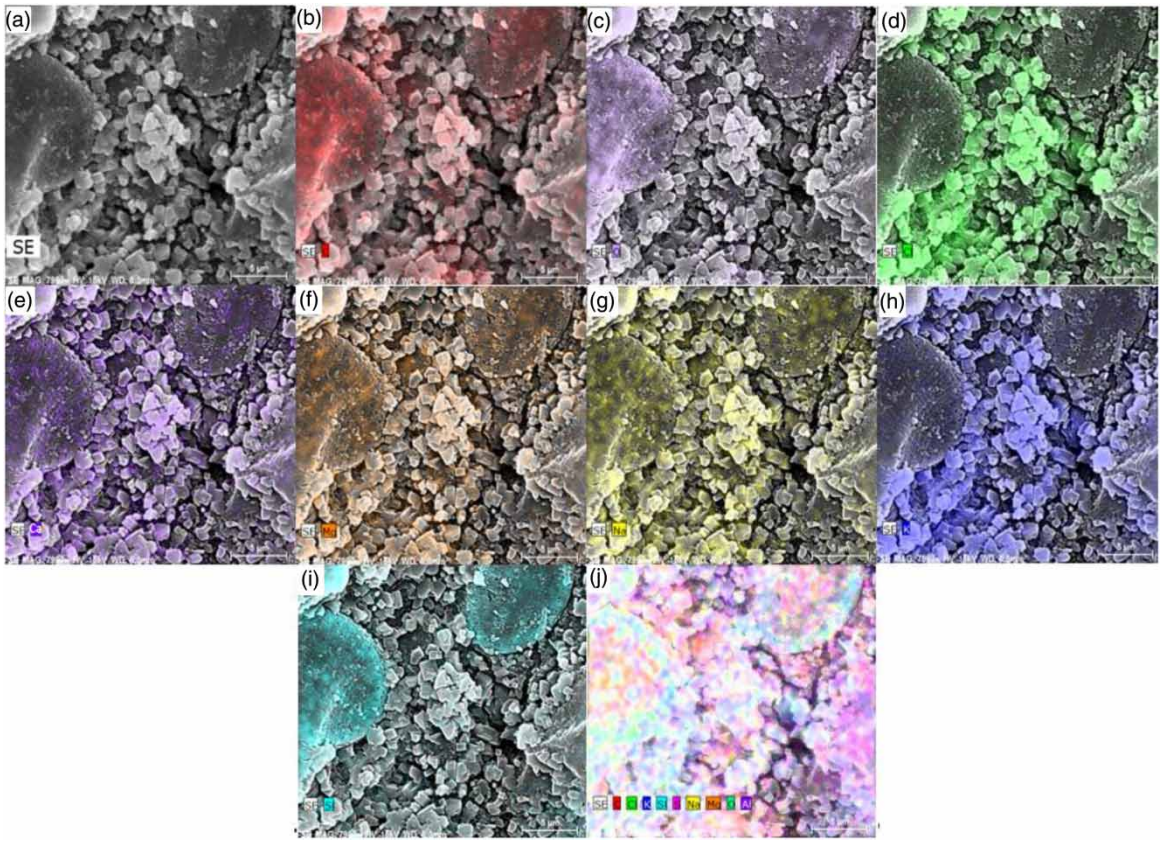

Figure 3 | (a) SEM image of the surface of MA material and its EDX analysis, (b) carbon (C) element, (c) oxygen (O) element, (d) chlorine (Cl) element, (e) calcium (Ca) element, (f) magnesium (Mg) element, (g) sodium (Na) element, (h) potassium (K) element, (i) silicon (Si) element, and (j) the image of combined elements.

Effect of pH

The effect of pH is one of the significant factors influencing the adsorptive removal of some pollutants from aqueous solutions. The solution pH influences the ionization of adsorbates and the functional groups that are present on the surface of the adsorbents. The removal percentage values were plotted against the corresponding initial pH values. Keeping in mind that the pK_a of DMP is 10.1 and pH_{zpc} of BCM adsorbent is 9.87, Figure 5 shows that at low pH values, from 1 to 2, the maximum removal efficiency is approximately 75% and it decreases to reach 30% at pH values higher than 5. This may be attributed to the decrease in the protonated functional groups and, as a result, the repulsion between the adsorbate and adsorbent surface increases. This is in line with the finding of Won *et al.* (2005).

Effect of adsorbent dosage

The effect of adsorbent mass loading on the removal of DMP from its solution which contains 20 mg/L initial concentrations at pH 2 was studied. Figure 6 shows that the removal percentage of DMP molecules increases and the adsorption capacity of BCM adsorbents decreases with the increase of adsorbent dosage. This is attributed to the increase of adsorption active sites (i.e., carbonyl and acetal functional groups) with the increase of the adsorbent mass. The highest DMP removal efficiency (100%) was achieved by using 150 ± 0.1 mg of BCM adsorbent.

Adsorption of DMP molecules

Figure 7 presents the adsorption isotherms of DMP using BCM adsorbent. The experimental data of DMP adsorption

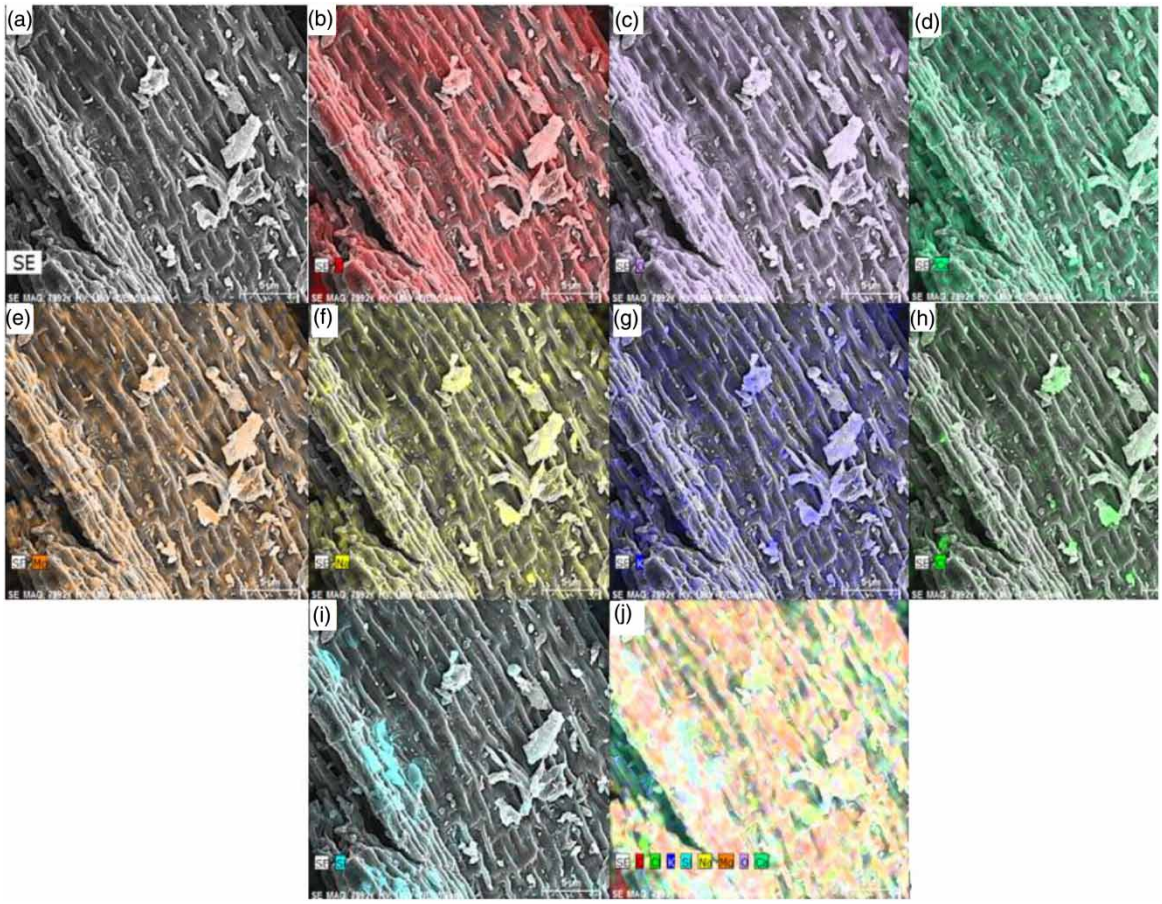

Figure 4 | (a) SEM image of the surface of BCM material and its EDX analysis, (b) carbon (C) element, (c) oxygen (O) element, (d) calcium (Ca) element, (e) magnesium (Mg) element, (f) sodium (Na) element, (g) potassium (K) element, (h) chlorine (Cl) element, (i) silicon (Si) element, and (j) the elements combined image.

Table 2 | The elements' percentage on the surface of macroalgae before and after carbonization

Element	MA element %	BCM element %
Carbon	35.56	61.78
Oxygen	12.81	33.85
Sodium	2.90	0.83
Magnesium	4.84	0.78
Chlorine	13.81	0.45
Potassium	22.23	0.22
Calcium	5.07	2.00
Silicon	0.20	0.07

were fitted with Freundlich, Langmuir, and Temkin adsorption isotherms. It is clearly shown that the experimental data fit the Freundlich model, whereas the difference between the experimental and the calculated q_e is the lowest. The obtained isotherm parameters from the linearized models are summarized in Table 3.

In the Freundlich model, the n value is obtained from the slope of the linear least square fit of $\ln(q_e)$ versus $\ln(C_e)$, while the K_F value is calculated from the intercept. Larger n and K_F values correspond, respectively, to greater heterogeneity on the adsorbent's surface and a higher adsorption capacity (Li *et al.* 2002). The n and K_F indicate that the adsorption of DMP phenolic compound is favorable on the BCM adsorbent. The squared correlation coefficient (R^2) value of the linearized Freundlich equation for DMP adsorption on BCM adsorbent is higher than the obtained R^2 values of the other linearized forms (i.e., Langmuir and Temkin isotherm equations). In addition, the SRE of fitting the experimental data with

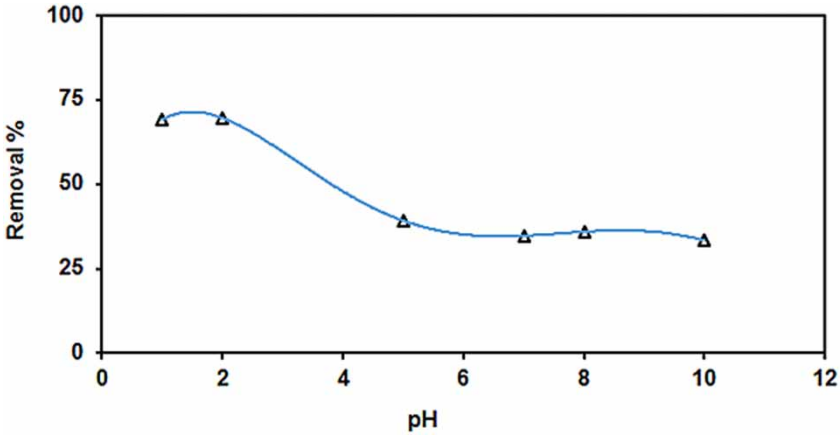

Figure 5 | Effect of pH on the removal percentage of DMP (10 mg/L) using 0.05 g BCM adsorbent at 24 ± 0.1 °C and contact time of 16 hours.

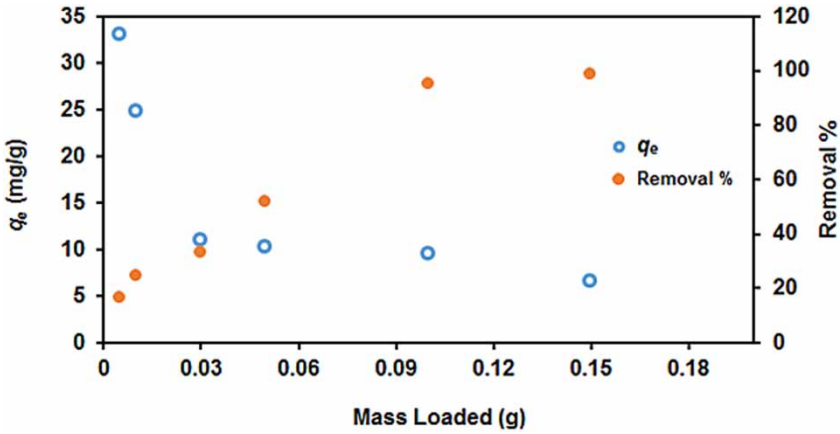

Figure 6 | The effect of adsorbent mass on the adsorption capacity (q_e) (primary y axis) and the removal percentage (secondary y axis) for DMP (20 mg/L) using BCM adsorbent at 24 ± 0.1 °C.

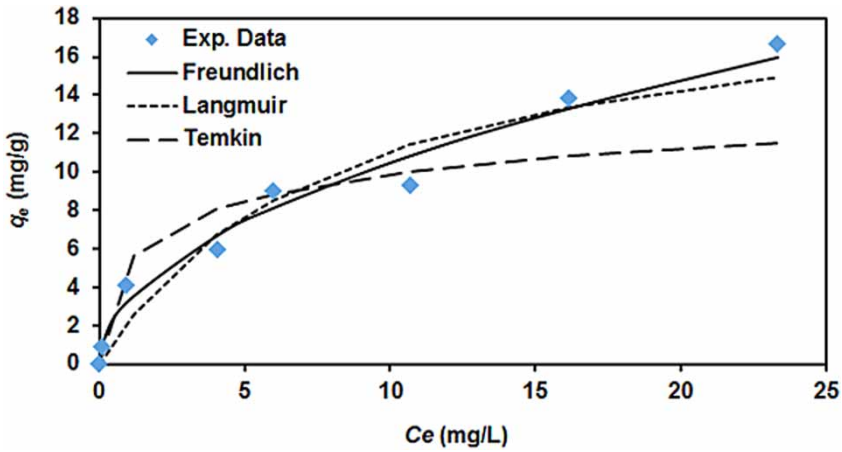

Figure 7 | The experimental data of the adsorption isotherms of DMP adsorption on BCM adsorbent at 24 ± 0.1 °C fitted with Freundlich, Langmuir, and Temkin models. The initial concentration of DMP ranges between 1 and 40 mg/L, pH of solutions is 2, BCM adsorbent mass is 50 ± 0.1 mg, and contact time is 16 hours.

Table 3 | Freundlich, Langmuir, and Temkin isotherm models' parameters for DMP adsorption on BCM adsorbents at 24 ± 0.1 °C

Freundlich	
n	1.93
K_F ((mg/g)(L/mg)$^{1/n}$)	3.18
R^2	0.9905
SRE	0.74
Langmuir	
b ((L/mg))	1.14
Q_o (mg/g)	9.37
R_L	0.02
R^2	0.9855
SRE	6.64
Temkin	
A_T (L/g)	1.01
b_T (J/mol)	916.88
R^2	0.8196
SRE	70.16

Freundlich is lower than those obtained by the fitting with the other linearized forms. However, R^2 of the linearized Langmuir isotherm model for DMP adsorption on BCM is also high, but lower than of R^2 of the linearized Freundlich equation. This indicates that the adsorption mechanism of DMP on the BCM adsorbent is mixed and dominated by a physisorption mechanism, and the hydrogen bonding, Van der Waals as well as acceptor–donor interactions between the adsorbent surface and the DMP adsorbate contribute to the adsorption process and these molecules form multi-layers on the adsorbent. In addition, the separation factor (R_L) value (shown in Table 3) for the adsorption of DMP on BCM is between 0 and 1 which indicates the adsorption is favorable. It has been also found that, within the experimental conditions, the maximum adsorption capacity is 17 mg/g for DMP (shown in Figure 7). This value is comparable with most of those reported in the literature (shown in Table 4). It has been found that the adsorption capacity of BCM is lower than the adsorption capacity of the standard activated charcoal (Jain *et al.* 2002) by eight times while it is higher than the adsorption capacity of K-FAU-X (zeolite) (Vittenet *et al.* 2014) by 28 times.

Table 4 | Adsorption capacity of different adsorbents for DMP phenolic compound

Adsorbent	Adsorption capacity (mg/g)	Reference
Standard activated charcoal	140.5	Jain *et al.* (2002)
Carbonaceous adsorbent	65.9	
Blast furnace sludge	21.9	
Blast furnace dust	18.3	
Blast furnace slag	Negligible	
K-FAU-X (zeolite)	0.6	Vittenet *et al.* (2014)
Coal fly ash	3.0	Batabyal *et al.* (1995)
BCM	17.0	This work

DMP adsorption kinetics

The mechanism of the adsorption can be explored by studying the adsorption kinetics. The results presented in Figure 8(a) show that the adsorption rates of DMP reach equilibrium within 9 hours. The experimental adsorption capacity ($q_{e,exp}$) for DMP on the BCM adsorbent is given in Table 5. It has been observed that DMP molecules are slowly adsorbed and reach equilibrium after 9 hours. The initial fast adsorption is attributed to the availability of a large number of active adsorption sites, while the slowness at which the maximum adsorption is reached is due to the occupied adsorption sites and the repulsion between the free adsorbate molecules in solution and the adsorbed molecules on the BCM adsorbent. The linear least square fits of $\ln(q_e - q_t)$ versus t and q_t versus $\ln(t)$ (shown in Figure 8(b) and 8(c)) with the adsorption data of DMP yield R^2 values of 0.973 and 0.907, respectively, that are lower than R^2 (0.990) value which is obtained from the linear least square fit of t/qt versus t (shown in Figure 8(d)). The calculated adsorption capacity ($q_{e\ pred}$) of DMP from the pseudo-first order and the Elovich kinetics deviates largely from the experimental adsorption capacity ($q_{e\ exp}$). However, SRE value of the linear least squares fits of $\frac{t}{q_t}$ versus t (see Table 5) is the lowest. This clearly reveals that the adsorption process follows pseudo-second order kinetics, and the chemisorption is involved in the adsorption mechanism.

Bearing in mind that the kinetic results fit into the pseudo-second order adsorption kinetics model for DMP on the adsorbent, the diffusion mechanism of these

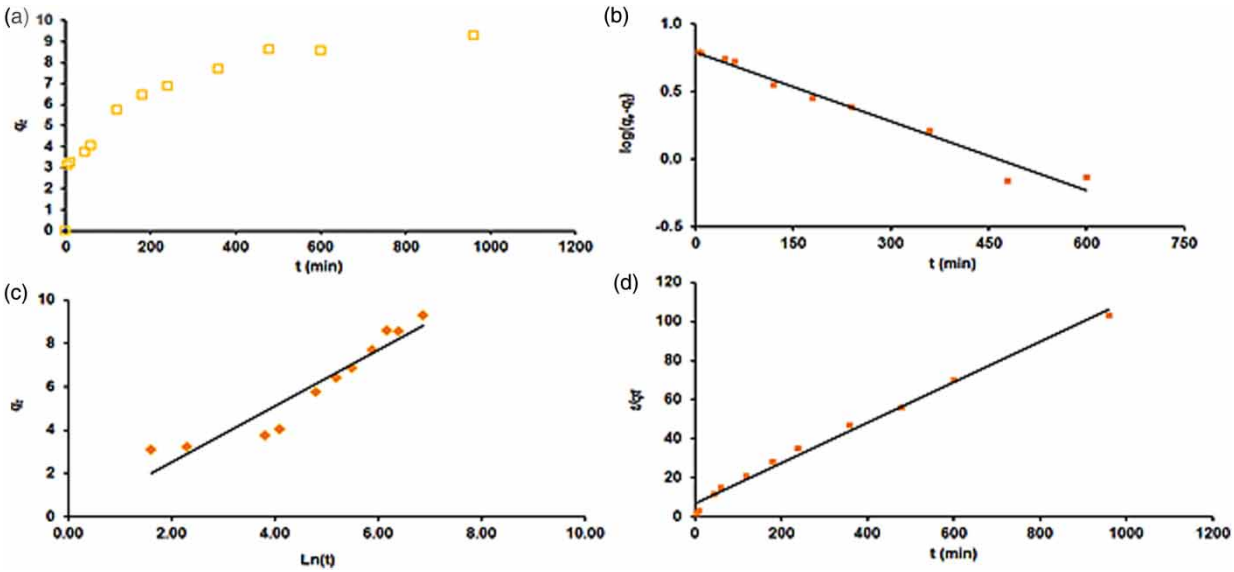

Figure 8 | (a) The effect of contact time on the adsorption capacity (q_t) of DMP (15 mg/L), (b) pseudo-first order, (c) Elovich, and (d) pseudo-second order sorption kinetics of DMP onto the BCM adsorbent at 24 ± 0.1 °C and pH equal to 2.

Table 5 | Pseudo-first order, pseudo-second order, and Elovich kinetics parameters for DMP adsorption on the BCM adsorbent

First order

$q_{e\ exp.}$	$q_{e\ pred.}$	k_1 (min^{-1})	R^2	SRE
9.3	6.2	0.0017	0.973	19.23

Second order

$q_{e\ exp.}$	$q_{e\ pred.}$	k_2 (g mg^{-1} min^{-1})	R^2	SRE
9.3	9.7	0.0015	0.9902	3.41

Elovich

$q_{e\ Exp.}$	a (mg g^{-1} min^{-1})	b (g mg^{-1})	R^2	SRE
9.3	1.2	0.7699	0.9071	19.86

molecules was tested and the influence of mass transfer resistance on their binding on the adsorbent was verified using intra-particle diffusion model (Weber & Morris 1963) through using Equation (15):

$$q_e = k_{id}t^{0.5} + C \quad (15)$$

where k_{id} is the intra-particle diffusion rate constant (mg g^{-1} min$^{-0.5}$), and C is a constant related to the thickness of the boundary layer (mg/g). k_{id} is obtained from the slope of the plot of q_t versus the square root of time.

Figure 9(a) shows the plot of q_t versus $t^{0.5}$ for DMP on BCM adsorbent. These results imply that the adsorption processes involve more than a single kinetic stage or sorption rate (Weber & Morris 1963). The first linear part (first stage) may be attributed to the mass transfer of adsorbate molecules across the boundary layer and intra-particle diffusion, which produces a delay in the adsorption process. The second stage is attributed to the diffusion through small pores, which is followed by the establishment of equilibrium. Table 6 summarizes the calculated values of the diffusion constants for DMP on the BCM adsorbent.

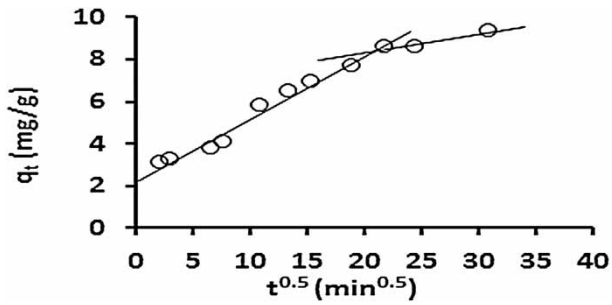

Figure 9 | Plot of q_t versus $t^{0.5}$ showing the two diffusion stages predicted by the diffusion model for DMP (15 mg/L) adsorption on the BCM adsorbent.

Table 6 | Intra-particle diffusion parameters for DMP molecules on the BCM adsorbent

Adsorbate	Parameters		
	K_{id}	C	R^2
DMP	0.24	2.66	0.95

Table 7 | Thermodynamic parameters for the adsorption of DMP on the BCM adsorbent

	DMP		
Temperature (K)	ΔG (kJ mol^{-1})	ΔH (kJ mol^{-1})	ΔS (kJ mol^{-1} K^{-1})
297	−5.84	108.10	0.38
303	−8.14		
308	−10.06		
313	−11.97		
323	−15.81		
333	−19.65		

Thermodynamics of DMP adsorption on BCM

For further investigation of the adsorption mechanism, the thermodynamic distribution coefficient (K_d) was calculated at different temperatures using Equation (16), the free energy (ΔG) was calculated using Equation (17), the enthalpy (ΔH) and entropy (ΔS) of the adsorption were calculated, respectively, from the obtained slope and the intercept of log K_d versus 1/T plots (Figure 10) using Equation (18), and the results are presented in Table 7.

$$K_d = \frac{q_e}{C_e} \tag{16}$$

$$\Delta G^o = RTlnK_d \tag{17}$$

$$\ln K_d = \frac{\Delta S^o}{R} - \frac{\Delta H^o}{RT} \tag{18}$$

The negative values of ΔG at all temperatures for the adsorption confirm that the adsorption process of DMP molecules on the BCM adsorbent is spontaneous and thermodynamically favorable. However, the positive value of ΔH and decreasing of ΔG value with increasing the temperature indicates that the adsorption process of DMP is endothermic. Zaghouane-Boudiaf & Boutahala (2011) reported that the adsorption process is physical if ΔG values range from −30 to 0 kJ mol^{-1} and it is a chemical process if ΔG values are between −400 and −80 kJ mol^{-1}. Also, the magnitude of ΔH gives an idea into the nature of the adsorption as to if it is physical or chemical. The physical adsorption evolves heat in the range of 2.1 and 20.9 kJ mol^{-1} while the chemical adsorption has a heat ranging between 80 and 400 kJ mol^{-1} (Saha & Chowdhury 2011). In this study, the calculated values of ΔG for DMP adsorption range between −19.65 and −5.84 kJ mol^{-1} and the ΔH value is 108.10 kJ mol^{-1}. These values indicate that the adsorption of DMP molecules involves a mixed adsorption mechanism and is dominated by physical adsorption. The small positive value of ΔS (0.38 kJ mol^{-1} K^{-1}) reflects the affinity of the adsorbent toward the adsorbate molecules and indicates that the randomness at the liquid/solid interface is increased.

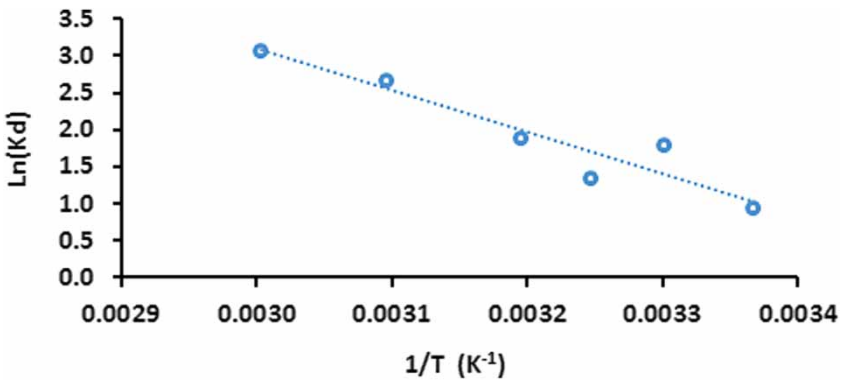

Figure 10 | Plot of ln K_d versus. 1/T for DMP adsorption on the BCM adsorbent.

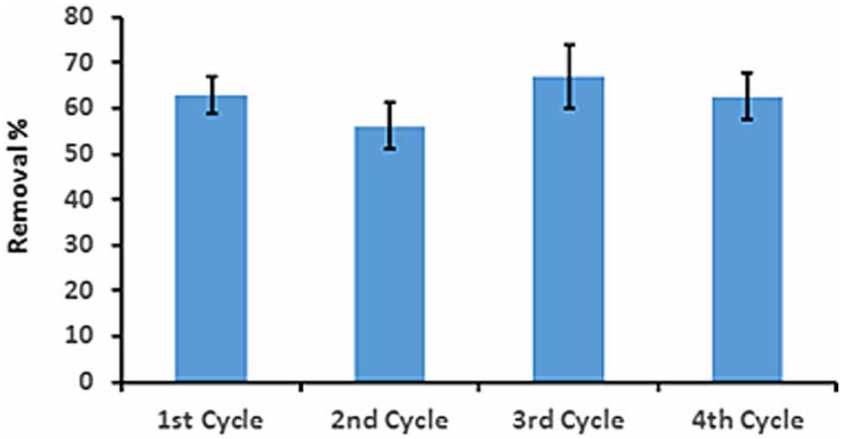

Figure 11 | The removal efficiency of DMP using BCM adsorbent, with error bars, after four adsorbent regeneration cycles.

REAL APPLICATION OF THE BCM ADSORBENT AND ITS REGENERATION

To approach the real application and since the cost-effectiveness and regeneration of the adsorbents are significant factors, the removal of DMP from seawater (pH = 7.80 and salinity = 41 g/kg) has been tested. 50 mL of seawater was spiked with 30 mg/L DMP and 200 ± 0.1 mg BCM adsorbent was added. DMP concentration before and after the adsorption was measured. It has been found that the prepared adsorbent removes around 60% of DMP from the tested seawater. Furthermore, the reusability of the prepared BCM adsorbent has been tested. The method for BCM adsorbent regeneration was very simple. After the completion of the adsorption experiments, the BCM adsorbent loaded with DMP was filtrated and washed three times with distilled water to remove the stacked salts then heated at 250 °C for 1 day in air to remove the adsorbed phenolic molecules. The regenerated BCM was reused for the next adsorption, and the successive adsorption-desorption cycles were repeated four times. As shown in Figure 11, BCM remains, within the experimental error, nearly unchanged in their ability for DMP adsorption for at least four cycles.

CONCLUSION

In this study, for the first time, biochar derived from *S. boveanum* macroalgae as an adsorbent has been prepared, characterized, then tested for the removal of 2,4-dimethylphenol from aqueous solution and its adsorption isotherms and kinetics were investigated. The carbonization improved the removal capability of the macroalgae adsorbent for DMP compound with removal efficiency up to 100%. The adsorption equilibrium results showed that the adsorption was attained through a mixed mechanism dominated by physisorption and followed by pseudo-second order kinetics. Also, the adsorption of DMP molecules is spontaneous and thermodynamically favorable with a negative value of ΔG. The adsorption process of these molecules is endothermic, while the positive value of ΔS reflects the affinity of the adsorbent toward the DMP adsorbate and indicates increasing of randomness at the liquid/solid interface. The findings in this study reveal that the biochar derived from BCM adsorbent can be used in the removal of DMP phenolic compound from high salinity seawater with removal efficiency up to 60% and reusability for at least four times.

ACKNOWLEDGEMENTS

The authors highly acknowledge the Center for Environment and Water (CEW) at King Fahd University of Petroleum and Minerals (KFUPM) for the support and funding this research study. The authors declare that there is no conflict of interest regarding the publication of this paper.

DATA AVAILABILITY STATEMENT

All relevant data are included in the paper or its Supplementary Information.

REFERENCES

Ahmaruzzaman, M. 2008 Adsorption of phenolic compounds on low-cost adsorbents: a review. *Advances in Colloid and Interface Science* **143**, 48–67. DOI.org /10.1016/j.cis.2008.07.002.

Ata, A., Nalcaci, O. O. & Ovez, B. 2012 Macro algae Gracilariaverrucosa as a biosorbent: a study of sorption mechanisms. *Algal Research* **1**, 194–204. DOI.org/10.1016/j.algal.2012.07.001.

Batabyal, D., Sahu, A. & Chaudhuri, S. K. 1995 Kinetics and mechanism of removal of 2,4-dimethyl phenol from aqueous solutions with coal fly ash. *Separations Technology* **5**, 179–186.

Chien, S. H. & Clayton, W. R. 1980 Application of Elovich equation to the kinetics of phosphate release and sorption on soils. *Soil Science Society of America Journal* **44**, 265–268. DOI.10.2136/sssaj1980.03615995004400020013x.

Cuizano, N., Llanos, B. & Navarro, A. E. 2009 Application of marine seaweeds as lead (II) biosorbent: analysis of the equilibrium state. *Revista de la Sociedad Química del Perú* **75**, 33–43. http://www.scielo.org.pe/pdf/rsqp/v75n1/a06v75n1.pdf

Eugenia, R., Pilar, R., Roberto, H. & Manuel, E. S. 2006 Biosorption of phenolic compounds by the brown alga *Sargassum muticum*. *Chemical Technology & Biotechnology* **81** (7), 1093–1099. doi.org/10.1002/jctb.1430

Freundlich, H. M. F. 1906 Über die Adsorption in Lösungen. (Adsorption in solution). *Zeitschrift für Physikalische Chemie* **57**, 385–471. DOI.org/10.1515/zpch-1907-5723.

Ho, Y. S. & McKay, G. 1998 A comparison of chermosorption kinetic models applied to pollutant removal on various sorbents. *Process Safety and Environmental Protection* **76** (4), 332–340. DOI.org/10.1205/095758298529696.

Jain, A. K., Suhas & Bhatnagar, A. 2002 Methylphenols removal from water by low-cost adsorbents. *Journal of Colloid and Interface Science* **251** (1), 39–45. https://doi.org/10.1006/jcis.2002.8395.

Lagergren, S. 1898 Zurtheorie der sogenannten adsorption gelösterstoffe. (To the theory of the so-called adsorption of dissolved materials). *Kungliga Svenska Vetenskapsakademiens Handlingar* **24** (4), 1–39.

Langmuir, I. 1916 The constitution and fundamental properties of solids and liquids. *Journal of the American Chemical Society* **38** (11), 2221–2295. DOI.10.1021/ja02242a004.

Laura, G. C. V., Neda, M., Miao, C., Debjani, M., Keith, E. T. & Nihar, B. 2016 A short review of techniques for phenol removal from wastewater. *Current Pollution Report* **2**, 157–167. DOI.org/10.1007/s40726-016-0035-3.

Li, L., Quinlivan, P. A. & Knappe, D. R. U. 2002 Effects of activated carbon surface chemistry and pore structure on the adsorption of organic contaminants from aqueous solution. *Carbon* **40**, 2085–2100. DOI.org/10.1016/S0008-6223(02)00069-6.

Li, X., Chen, S., Fan, X., Quan, X., Tan, F., Zhang, Y. & Gao, J. 2015 Adsorption of ciprofloxacin, bisphenol and 2-chlorophenol on electro spun carbon nanofibers: in comparison with powder activated carbon. *Journal of Colloid and Interface Science* **447**, 120–127. DOI.org/10.1016/j.jcis.2015.01.042.

Mohammadi, S., Kargari, A., Sanaeepur, H., Abbassian, K., Najafi, A. & Mofarrah, E. 2015 Phenol removal from industrial wastewaters: a short review. *Desalination and Water Treatment* **53**, 2215–2234. DOI.org/10.1080/19443994.2014.883327.

Navarro, A. E., Cuizano, N., Portales, R. & Llanos, B. 2008 Adsorptive removal of 2-nitrophenol and 2-chlorophenol by cross-linked algae from aqueous solutions. *Separation Science and Technology* **43**, 3183–3199. DOI.org/10.1080/01496390802221642.

Nazal, K. 2019 *Marine Algae Bioadsorbents for Adsorptive Removal of Heavy Metals*. In: *Advanced Sorption Process Applications* (S. Edebali, ed.). IntechOpen. DOI: 10.5772/intechopen.80850.

Podgorskii, V. S., Kasatkina, T. P. & Lozovaia, O. G. 2004 Yeasts – biosorbents of heavy metals. *Mikrobiolohichnyi Zurnal* **66**, 91–103. Pubmed ID 15104060.

Saha, P. & Chowdhury, S. 2011 Insight into adsorption thermodynamics. In: *Thermodynamics* (M. Tadashi, ed.). InTech. Available from: http://www.intechopen.com/books/thermodynamics/insight-intoadsorption-thermodynamics.

Sekkal, M., Huvenne, J., Legrand, P., Sombret, B., Mollet, J., Mouradi-Givernaud, A. & Verdus, M. 1993 Direct structural identification of polysaccharides from red algae by FTIR micro spectrometry I: localization of agar in Gracilariaverrucosa sections. *Microchimica Acta* **112** (1–4), 1–10. DOI.org/10.1007/BF01243315.

Snoeyink, V. L., McCreary, J. J. & Murin, C. J. 1997 Carbon adsorption of traces organic compounds. Municipal Research Lab, Office of Research and Development, U.S. Environmental Protection Agency, Cincinnati, Ohio. Washington, DC, EPA/600/2-77/223.

Sun, X., Wang, C., Li, Y., Wang, W. & We, J. 2015 Treatment of phenolic wastewater by combined UF and NF/RO processes. *Desalination* **355**, 68–74. DOI.org/10.1016/j.desal.2014.10.018.

Temkin, M. I. & Pyzhev, V. 1940 Kinetics of ammonia synthesis on promoted iron catalyst. *Acta Physicochimica USSR* **12**, 327–356. https://ci.nii.ac.jp/naid/20000744365.en.tsv

Vidic, R. D., Suidan, M. T. & Brenner, R. C. 1993 Oxidative coupling of phenols on activated carbon: impact on

adsorption equilibrium. *Environmental Science and Technology* **27** (10), 2079–2085.

Vittenet, J., Rodriguez, J., Petit, E., Cot, D., Mendret, J., Galarneau, A. & Brosillon, S. 2014 Removal of 2,4-dimethylphenol pollutant in water by ozonation catalyzed by SOD, LTA, FAU-X zeolites particles obtained by pseudomorphic transformation (binderless). *Microporous and Mesoporous Materials* **189**, 200–209.

Weber Jr, W. J. & Morris, J. C. 1963 Kinetics of adsorption on carbon from solution. *Journal of the Sanitary Engineering Division* **89**, 31–60.

Won, S. W., Choi, S. B. & Yun, Y. S. 2005 Interaction between protonated waste biomass of Corynebacteriumglutamicum and anionic dye Reactive Red 4. *Colloids Surfaces A: Physicochemical and Engineering Aspects* **262**, 175–180. DOI.10.1016/j.colsurfa.2005.04.028.

Zaghouane-Boudiaf, H. & Boutahala, M. 2011 Adsorption of 2,4,5-trichlorophenol by organo-montmorillonites from aqueous solutions: kinetics and equilibrium studies. *Chemical Engineering Journal* **170**, 120–126. DOI.org/10.1016/j.cej.2011.03.039.

First received 23 October 2019; accepted in revised form 18 May 2020. Available online 8 July 2020